Lasers in Manufacturing Conference 2017

Surface structuring with a 500 W picosecond laser

Sebastian Faas[a,*], Corrado Sciancalepore[b], Rudolf Weber[a], Luca Romoli[c], and Thomas Graf[a]

[a]*Institut für Strahlwerkzeuge (IFSW), University of Stuttgart, Pfaffenwaldring 43, 70569 Stuttgart, Germany*
[b]*National Interuniversity Consortium of Materials Science and Technology (INSTM-Research Unit of Parma), Florence, Italy*
[c]*Department of Engineering and Architecture, University of Parma, 43124 Parma, Italy*

Abstract

The surface structure has a significant influence on the wetting behavior of the surface. To obtain superhydrophobic surfaces several methods of surface texturation exist. Laser-induced periodic surface structures (LIPSS) are commonly used for surface structuring. LIPSS are produced with low fluences close to the ablation threshold. Processing with fluences well above the ablation threshold can lead to a surface which is covered with so-called bumps. Bumps are hilly structures with a size in the range of a few microns and can also be covered with ripples. Both surface topographies were produced within a pre-testing phase to test the wettability. Additionally, the influence of the cleaning agent was investigated for both surface structures. A 500 W laser with a wavelength of 1030 nm, a repetition rate of 300 kHz and a pulse duration of 8 ps was used for upscaling surface texturing experiments of AISI 316L and AISI L7. For a fluence close to the ablation threshold the number of pulses per spot was varied to increase the heat input resulting in different surface structures. The wetting behavior of these structuring strategies was compared by measuring the static contact angle. Surface structuring rates up to 500 mm²/s were realized.

Keywords: Micro Processing; Surface Functionalization; Heat Accumulation.

* Corresponding author. Tel.: +49-711-685-66881; Fax: +49-711-685-59759.
E-mail address: sebastian.faas@ifsw.uni-stuttgart.de.

1. Introduction

According to Loo et al., 2012 as well as Boinovich and Emelyanenko, 2008 functionalized surfaces are expected to be used widely e. g. in the field of medical technology, food and home-appliance industries. Since the laser is a suitable tool to produce functionalized surfaces the research activities have grown fast since the year 2000, see Bonse et al., 2017.

1.1. Basic low-average power investigations

A laser with an average power of P_{av} = 12 W, a wavelength of λ_0 = 1064 nm, a pulse duration of τ_0 = 10 ps, and a repetition rate of f_0 = 300 kHz was used to structure rolled non-treated AISI 304. Two different structures were created to test the fundamental wetting behavior of both surface topographies. The surface topographies for both types can be seen in Fig. 1. In Fig. 2(a) ripples and in Fig. 2(b) bumps with ripples on top can be seen.

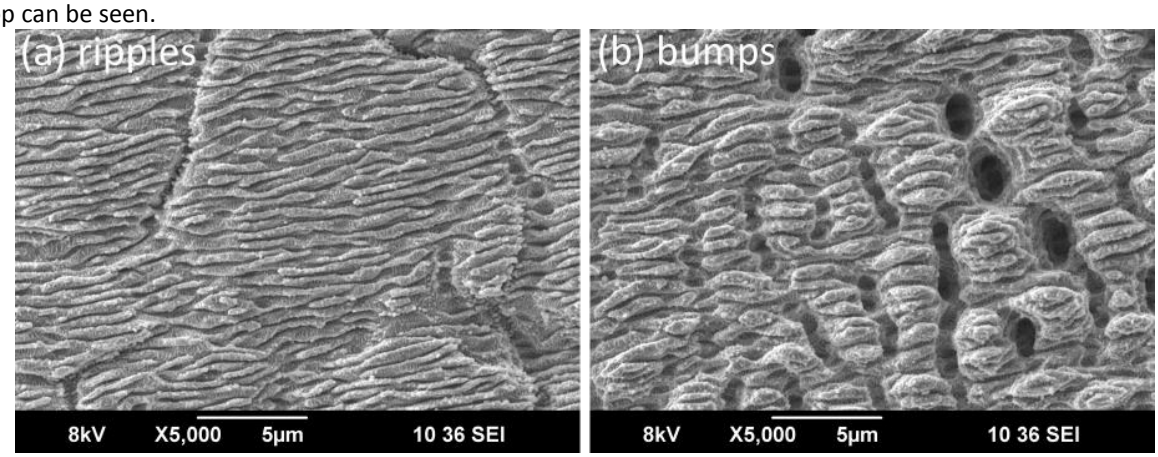

Fig. 1. SEM images of structured surface areas on rolled non-treated AISI 304. Laser parameter: P_{av} = 12 W, λ_0 = 1064 nm, f_0 = 300 kHz, d_f = 20 µm, d_l = 10 µm, (a) Ripples created with E_P = 1.8 µJ , and v = 0.5 m/s, (b) Bumps created with E_P = 20 µJ, and v = 0.5 m/s.

Additionally, the influence of the cleaning agent was investigated. Acetone, ethanol, denatured ethanol, and dry air were used for sample cleaning after measuring the static contact angle (SCA). The measurements were performed by hand using a Transferpette S (Brand GmbH + Co KG, Germany). The pictures of the droplet on the surface were analyzed with imageJ to determine the SCA. The first measurement of the SCA took place immediately after the processing. After cleaning with an individual cleaning agent all samples were stored in ambient air at room temperature. Before all following measurements the structured areas were cleaned with a dry air flow to remove dust from the surface. The results can be seen in Fig. 2. While reaching the steady state SCA there is a small difference between the cleaning agents. The non-existence of a long-term effect can be seen easily. Obviously, the cleaning agent had no noticeable effect on the wetting properties of the surface.

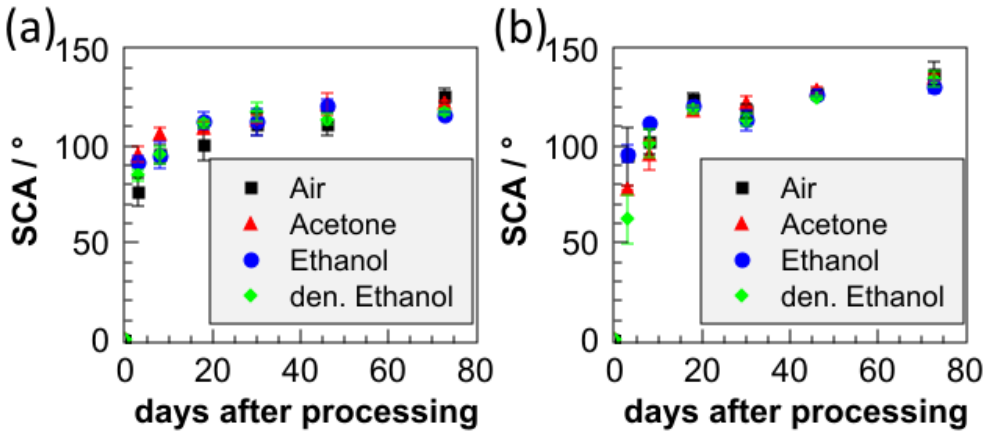

Fig. 2. SCA as a function of days after processing when using different cleaning agents for (a) ripples and (b) bumps.

As Gemini et al., 2013 report one of the major future challenges is the upscaling of the laser surface structuring process to large areas of several square meters. To reach high structuring rates laser systems with high average power are necessary. The average laser power $P_{av} = E_P \cdot f$ can be increased by increasing either the pulse energy E_P or the pulse repetition rate f.

2. High-average power experiments

The laser system used within this study was reported in Negel et al., 2013. The wavelength of the laser is λ=1030 nm, the repetition rate of the laser was f=300 kHz, and the average laser power was P_{av} = 500 W corresponding to a pulse energy of E_P = 1.67 mJ. The laser beam was linearly polarized. A fast scanner system equipped with an F-Theta lens having a focal length of 160 mm was used to move the beam over the surface of the samples at about normal incidence over the whole processed field. During the experiments the focal position was about 25 mm above the workpiece surface. A laser spot diameter of about d_f = 0.8 mm onto the surface of the sample was calculated using the ABCD-formalism. This yielded a calculated fluence of 0.33 J/cm^2 which is close to the ablation threshold. Additionally, the feed was in all experiments perpendicular to the direction of the polarization.

In this experiment we used two different materials. On the one hand we used AISI 316L square plates having a thickness of 2 mm and a surface area of 50 x 50 mm². Two types of surfaces were used: one with a surface roughness of Ra = 0.8 µm and one with a surface roughness of Ra = 1.6 µm. On the other hand we used AISI L7 which is a plastic molding steel and does not belong to the group of stainless steels. The scanning strategy was to produce the structures with parallel lines. The distance between adjacent lines was d_l = 50 µm. Feed rates from v_{min} = 1 m/s to v_{max} = 10 m/s were used for surface structuring. The irradiated samples were examined by scanning electron microscopy (SEM).

The wetting behavior of the surfaces was evaluated by means of SCA measurements using the sessile drop method. Contact angles with drops of deionized water (drop volume 1-4 µl) were recorded as a function of time, with the contact angle meter OCA 20 (DataPhysics Instruments GmbH, Germany) under room condition.

After each measurement, the samples were ultrasonic cleaned in ethanol, washed with fresh ethanol, dried in vacuum and stored in a closed box at room temperature and pressure.

3. Experimental Results

The SEM images of the structured areas on AISI 316L having an initial surface roughness of Ra = 0.8 µm are shown in Fig. 1. Referring to Bonse et al., 2017 the ripples in this study can be identified as low spatial frequency LIPSS (LSFL) (Fig. 3 (a)-(b).With lower feed rates the surface becomes rougher showing so-called bumps (Fig. 3 (c)-(d). Bauer et al., 2015 report on a critical surface temperature T_{crit}=607 °C where the transition takes place from a smooth and high reflective surface to a dark and bumpy surface. These bumps are in the range of few microns and are covered with LSFL and thus it can be called a double-scale structure, see Wu et al., 2009. According to Bizi-Bandoki et al., 2011 , a double scale structure is supposed to be a suitable structure to reach superhydrophobicity.

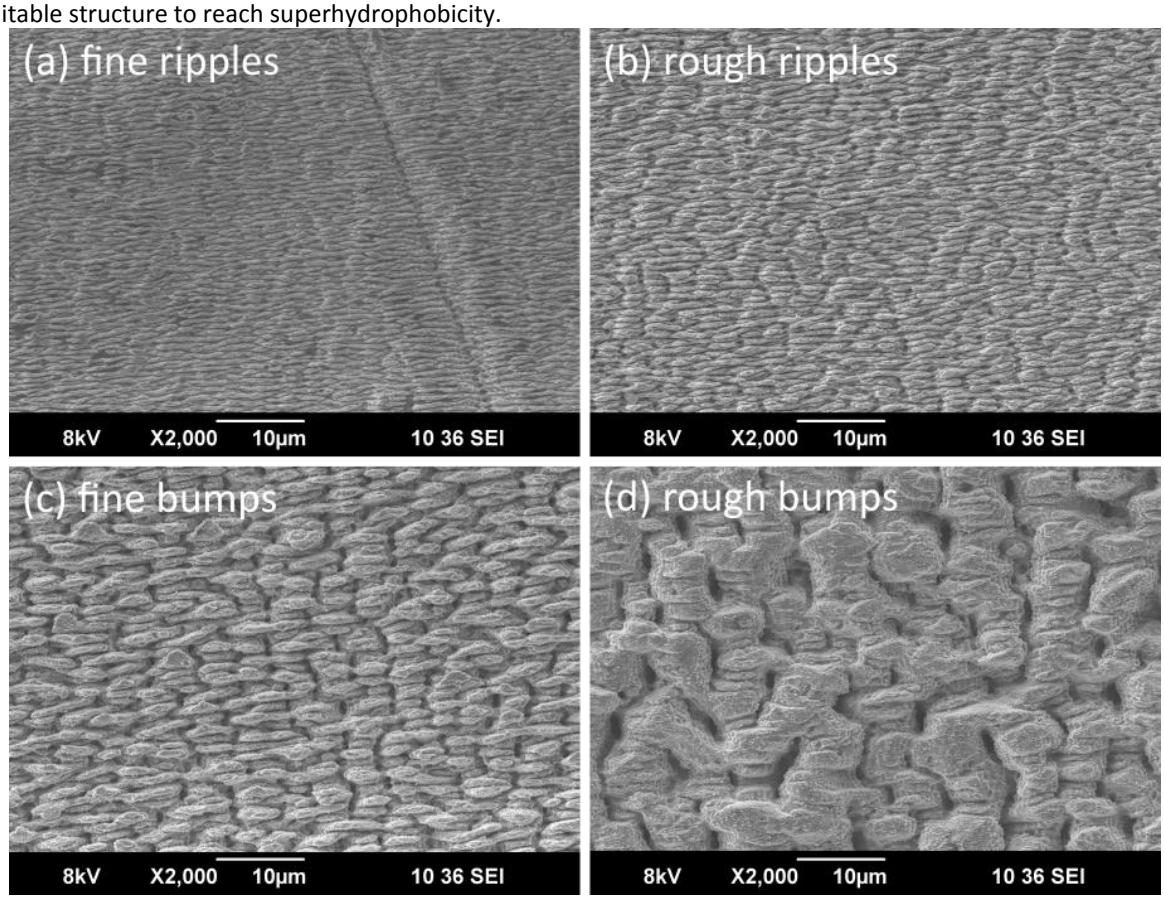

Fig. 3. SEM images of structured surface areas on AISI 316L having an initial roughness Ra=0.8 µm. Laser parameter: P_{av} = 500 W, λ=1030 nm, f=300 kHz, E_P =1.67 mJ, d_f=0.8 mm, d_l=50 µm, (a) v=10.0 m/s, (b) v=5.0 m/s, (c) v=2.5 m/s, (d) v=1.0 m/s.

The structures were analyzed with a laser scanning microscope. In Fig. 4 the 3D surface of AISI 316L having an initial surface roughness of Ra = 0.8 µm structured with a feed rate of v_{min} = 1.0 m/s (Fig. 4(a)) and v_{max} = 10.0 m/s (Fig. 4(b)) are shown. For the higher feed rate the scratches due to polishing of the sample before processing can be seen in Fig. 4(b). The process itself was not capable to cover these scratches and thus the scratches have a big influence on the surface characteristics. For the lower feed rate bumps were generated within the process (Fig. 4(a)). The scratches due to polishing could not be identified clearly. Thus, this process seems to be suitable to cover irregularities of the initial surface in the range of few microns.

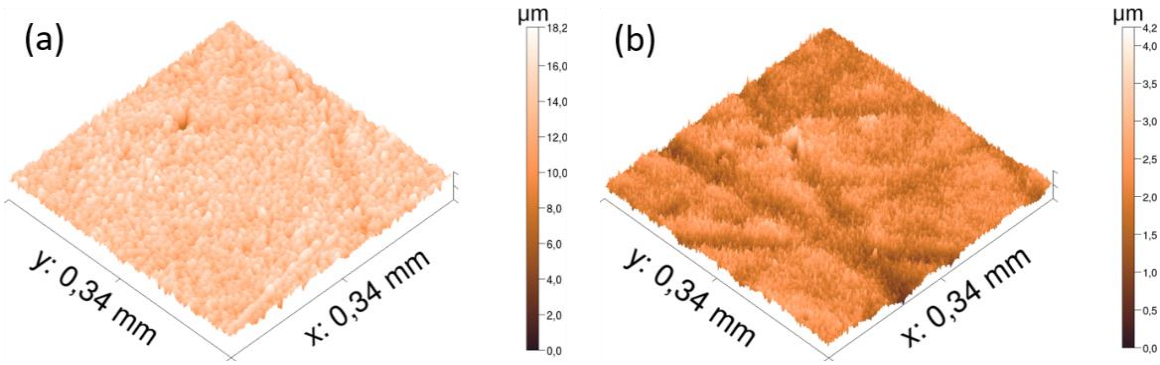

Fig. 4. 3D measurement of structured surface areas on AISI 316L having an initial roughness Ra=0.8 µm. Laser parameter: P_{av} = 500 W, λ = 1030 nm, f = 300 kHz, E_P = 1.67 mJ, d_f = 0.8 mm, d_l = 50 µm, (a) v = 1.0 m/s, (b) v = 10.0 m/s.

Table 1. Surface characteristics of the structured areas determined with a laser scanning microscope.

Sample	S_a	S_q	S_z
AISI 316L Ra=0.8 µm			
v=1.0 m/s	1.156 µm	1.478 µm	23.106 µm
v=2.5 m/s	0.620 µm	0.777 µm	10.083 µm
v=5.0 m/s	0.298 µm	0.377 µm	3.877 µm
v=10.0 m/s	0.321 µm	0.406 µm	4.241 µm
AISI 316L Ra=1.6 µm			
v=1.0 m/s	1.420 µm	1.776 µm	19.657 µm
v=2.5 m/s	0.729 µm	0.915 µm	9.605 µm
v=5.0 m/s	0.564 µm	0.730 µm	7.959 µm
v=10.0 m/s	0.771 µm	0.951 µm	7.505 µm
AISI L7			
v=1.0 m/s	3.653 µm	4.603 µm	33.42 µm
v=2.0 m/s	3.449 µm	4.497 µm	32.904 µm
v=3.0 m/s	1.426 µm	1.866 µm	26.128 µm
v=5.0 m/s	2.881 µm	3.564 µm	25.471 µm
v=10.0 m/s	3.623 µm	4.343 µm	23.719 µm

The surface roughness was determined from the 3D measurements. The arithmetical mean height of the surface S_a, the root mean square height of the surface S_q, and the maximum height of the surface are listed in Table 1 for the different processing parameters. Generally, an increasing roughness for lower feed rates was measured. However, the AISI 316L samples did not show this correlation. The smoothest surface was produced with a feed rate of v = 5.0 m/s for both initial roughnesses of the workpiece. A reason for this could be the scratches due to polishing of the samples which can be seen in Fig. 4(b).

The results of the CA measurements are listed in Table 2. Each CA value is the average of three measurements. All structured areas show a hydrophobic behavior. Surface structuring rates up from 50 mm²/s (v = 1 m/s) to 500 mm²/s (v = 10 m/s) were realized and are listed in Table 2. The type of structure for all structured areas is also listed in Table 2. For the AISI L7 samples the roughness was too pronounced to evaluate the final surface structure and thus it is not applicable (n/a). Comparing the wetting behavior of the structured areas listed in Table 2 there is no sharp transition from ripples regime to bumps regime which occurs between 5.0 m/s and 2.5 m/s. One reason could be the influence of the irregularities of the initial surface. On the other hand Weber et al., 2014 and further Weber et al., 2017 report on the major influence of heat accumulation to the process itself as well as to processing quality. Additionally, Bauer et al., 2015 report also on a strong oxidized surface if the surface temperature exceeds T_{crit} during processing. Since oxidization changes the chemical composition of the workpiece surface the wetting behavior can also change.

Table 2. Static Contact angle (SCA) for all structured areas depending on the aging time. Note that for *) no CA could be determined due to likely surface contamination.

Aging time	20 days	47 days	107 days		
Sample	SCA	SCA	SCA	Type of structure	Structuring rate
AISI 316L Ra=0.8 µm					
v=1.0 m/s	64° +/- 6°	107° +/- 1°	141° +/- 5°	rough bumps	50 mm²/s
v=2.5 m/s	143° +/- 1°	135° +/- 1°	137° +/- 2°	fine bumps	125 mm²/s
v=5.0 m/s	123° +/- 5°	137° +/- 1°	139° +/- 2°	rough ripples	250 mm²/s
v=10.0 m/s	134° +/- 1°	137° +/- 2°	137° +/- 3°	fine ripples	500 mm²/s
AISI 316L Ra=1.6 µm					
v=1.0 m/s	64° +/- 2°	111° +/- 4°	*)	rough bumps	50 mm²/s
v=2.5 m/s	104° +/- 7°	137° +/- 2°	143° +/- 2°	fine bumps	125 mm²/s
v=5.0 m/s	131° +/- 5°	137° +/- 1°	143° +/- 3°	rough ripples	250 mm²/s
v=10.0 m/s	136° +/- 1°	135° +/- 1°	136° +/- 3°	fine ripples	500 mm²/s
AISI L7					
v=1.0 m/s	109° +/- 5°	159° +/- 1°	152° +/- 2°	N/A	50 mm²/s
v=2.0 m/s	94° +/- 1°	144° +/- 1°	143° +/- 1°	N/A	100 mm²/s
v=3.0 m/s	95° +/- 2°	140° +/- 3°	146° +/- 3°	N/A	150 mm²/s
v=5.0 m/s	108° +/- 4°	145° +/- 1°	145° +/- 1°	N/A	250 mm²/s
v=10.0 m/s	120° +/- 3°	139° +/- 1°	138° +/- 1°	N/A	500 mm²/s

4. Conclusion and Outlook

Hydrophobic surfaces on AISI 316L and AISI L7 were produced with structuring rates up to 500 mm²/s. Several morphologies were obtained when varying the number of pulses per spot. The more pulses per spot the higher the heat input per area resulting in rougher surface structures. Based on their wetting behavior some of the structures presented in this study will be used to investigate the bacterial growth on them. Further investigations will take into account the influence of the repetition rate as well as using higher pulse energies. Additionally, the influence of the heat accumulation will be investigated. Furthermore, the long term stability of the structured areas will be under investigation.

Acknowledgements

This project has received funding from the European Union´s Horizon 2020 Research and Innovation Programme under Grant Agreement No 687613.

References

Bauer, Franziska; Michalowski, Andreas; Kiedrowski, Thomas; Nolte, Stefan, 2015. Heat accumulation in ultra-short pulsed scanning laser ablation of metals, Optics express 23 2, p. 1035

Bizi-Bandoki, P.; Benayoun, S.; Valette, S.; Beaugiraud, B.; Audouard, E., 2011. Modifications of roughness and wettability properties of metals induced by femtosecond laser treatment, Applied Surface Science 257 12, p. 5213

Boinovich, L. B.; Emelyanenko, A. M., 2008. Hydrophobic materials and coatings. Principles of design, properties and applications, Russ. Chem. Rev. 77 7, p. 583

Bonse, Jorn; Hohm, Sandra; Kirner, Sabrina V.; Rosenfeld, Arkadi; Kruger, Jorg, 2017. Laser-Induced Periodic Surface Structures— A Scientific Evergreen, IEEE J. Select. Topics Quantum Electron. 23 3, p. 1

Gemini, Laura; Faucon, Marc; Romoli, Luca; Kling, Rainer. High throughput laser texturing of super-hydrophobic surfaces on steel, 100921G

Loo, Ching-Yee; Young, Paul M.; Lee, Wing-Hin; Cavaliere, Rosalia; Whitchurch, Cynthia B.; Rohanizadeh, Ramin, 2012. Superhydrophobic, nanotextured polyvinyl chloride films for delaying Pseudomonas aeruginosa attachment to intubation tubes and medical plastics, Acta biomaterialia 8 5, p. 1881

Negel, Jan-Philipp; Voss, Andreas; Abdou Ahmed, Marwan; Bauer, Dominik; Sutter, Dirk; Killi, Alexander; Graf, Thomas, 2013. 1.1 kW average output power from a thin-disk multipass amplifier for ultrashort laser pulses, Optics letters 38 24, p. 5442

Weber, Rudolf; Graf, Thomas; Berger, Peter; Onuseit, Volkher; Wiedenmann, Margit; Freitag, Christian; Feuer, Anne, 2014. Heat accumulation during pulsed laser materials processing, Optics express 22 9, p. 11312

Weber, Rudolf; Graf, Thomas; Freitag, Christian; Feuer, Anne; Kononenko, Taras; Konov, Vitaly I., 2017. Processing constraints resulting from heat accumulation during pulsed and repetitive laser materials processing, Optics express 25 4, p. 3966

Wu, Bo; Zhou, Ming; Li, Jian; Ye, Xia; Li, Gang; Cai, Lan, 2009. Superhydrophobic surfaces fabricated by microstructuring of stainless steel using a femtosecond laser, Applied Surface Science 256 1, p. 61